J. Cell. Mol. Med. Vol 16, No 11, 2012 pp. 2637-2646

Expression of microRNA-122 contributes to apoptosis in H9C2 myocytes

Xiaoyan Huang [a], Fang Huang [a], Deye Yang [a, *], Fengquan Dong [a], Xiangxiang Shi [a], Hongyu Wang [c], Xi Zhou [a], Suyun Wang [a], Shengchuan Dai [b]

[a] *Division of Cardiology, The First Affiliated Hospital of Wenzhou Medical College, Wenzhou, China*
[b] *Division of Cardiology, Cardiovascular Institute, University of Pittsburgh Medical Center, Pittsburgh, PA, USA*
[c] *Department of Vascular Medicine, Shougang Hospital, Peking University, Beijing, China*

Received: November 6, 2011; Accepted: March 20, 2012

Abstract

The microRNAs (miRNAs) can post-transcriptionally regulate gene expression and heart development. The Pax-8 gene knockout mice have apparent heart abnormalities. This study investigated the role of miRNAs in regulation of cardiac apoptosis and development in the knockout mice. MicroRNA microarrays demonstrated differential expression of microRNAs between Pax-8$^{-/-}$ and Pax-8$^{+/-}$ mice, confirmed by real-time PCR. The miR-122 was up-regulated by 1.92 folds in Pax-8$^{-/-}$ mice. There were ventricular septum defects in Pax-8$^{-/-}$ mice, and increased numbers of apoptotic cells in the left ventricular wall and interventricular septum in Pax-8$^{-/-}$ mice. In H9C2 myocytes, treatment with miR-122 mimics or miR-122 inhibitor affects the expression of CCK-8 and activity of Caspase-3. The miR-122 is up-regulated in the myocytes of Pax-8$^{-/-}$ mice and may participate in the apoptotic gene expression and pathogenesis of heart development defect.

Keywords: miR-122 • differential expression • ventricular septum defect • apoptosis • HAND2

Introduction

Non-coding microRNAs are small and endogenous RNAs that regulate gene expression [1–3]. The microRNAs can repress translation or promote cleavage of mRNA by targeting the 3′ non-coding region (3′-UTR) [4], achieving the post-transcriptional gene silencing effect. The microRNAs function in the regulation of development, cell proliferation, apoptosis and haematopoiesis [5–7]. The microRNAs are highly expressed in the heart and regulate heart development [8, 9].

Congenital heart disease (CHD) affects about 1% of newborn children in the world and results in high morbidity and mortality, especially in infants under 1 year of age [10]. The CHD represents the largest class of birth defects and accounts for 25% of all human congenital abnormalities [11]. Ventricular septum defect (VSD) is a common CHD, however, it's specific mechanism and risk factors are yet to be clarified.

Paired box gene 8, also known as Pax-8, is a protein which in humans is encoded by the Pax-8 gene. This gene is a member of the paired box (Pax) family of transcription factors. Members of this gene family typically encode proteins which contain a paired box domain, an octapeptide and a paired-type homeodomain. This nuclear protein is involved in thyroid follicular cell development and expression of thyroid-specific genes. Pax-8 gene knockout mice develop various forms of heart abnormalities, particularly those similar to VSD and spheroidal heart with left ventricle enlargement. Apoptosis cells prevail in left ventricular wall and interventricular septum in Pax-8 knockout mice. In addition, myocytes apoptosis increases after down-regulation of Pax-8 gene *in vitro* [12]. Therefore, we investigated whether miRNAs are involved in the cardiac structural abnormalities of Pax-8 knockout mice.

Materials and methods

Establishment and identification of Pax-8 knockout mice

Homozygote (Pax-8$^{-/-}$) and heterozygote (Pax-8$^{+/-}$) Pax-8 knockout mice were generated as reported previously. Their genotypes were

*Correspondence to: Professor Deye YANG,
Division of Cardiology, the First Affiliated Hospital, Institute for Cardiovascular Biology & Gene, Wenzhou Medical College, Wenzhou 325000, China.
Tel.: +86-577-88658875
Fax: +86-577-88069555
E-mail: deyeyang203@hotmail.com

doi: 10.1111/j.1582-4934.2012.01577.x

identified by PCR. The following primers were used for genotype identification of Pax-8: forward primer 5′-GGATGTGGAATGTGTGCGAGG-3′, 5′-GCTAAGAGAAGGTGGATGAGAG-3′, and reverse primer 5′-GATGCTGCCAGTCTCGTAG-3′. The DNA was denaturated at 94°C for 5 min., followed by 25 cycles of denaturation for 15 sec., at 94°C, annealing for 15 sec., at 60°C, extension of 30 sec. at 72°C.

microRNA microarray analysis

Total RNA was isolated from the mice heart of experimental and control groups with TRIZOL reagent (Invitrogen, Carlsbad, CA, USA). The RNA quality was identified by ultraviolet absorption test and formaldehyde denatured agarose gel electrophoresis. The microRNAs were isolated, purified and labelled with Cy3, then hybridized with the miRNA oligonucleotide microarray (Agilent, Santa Clara, CA, USA). The gel was scanned by an Agilent scanner, and the density was determined by Feature Extraction software (Scan resolution 5 μm, PMT 100% and 5%). Mean value ratio between the two groups more than 2 or less than 0.5 is considered significantly up-regulated or down-regulated.

Real-time PCR analysis

Reverse transcription of miRNAs was performed with the miScription Reverse Transcription Kit (Qiagen, Valencio, CA, USA) according to manufacturer's recommendations. The PCR reaction was performed with the ABI7300. The relative amount of each miRNA was normalized to the U6 RNA using the equation $2^{-\Delta CT}$, where $\Delta CT = (CT_{miRNA-CTU6RNA})$ (CT was indicated to the cycles required by fluorescence signal intensity reaching to the threshold value in PCR amplification process). The miRNA specific real-time quantitative RT-PCR primers (Table 1, synthesized by Invitrogen) were used in the real-time PCR together with the miScript Universal Primer which was included in the kit. The test was repeated three times.

Table 1 The miRNA specific primers

miRNA	Primer sequence
mmu-miR-148a*	tcagtgcactacagaactttgt
mmu-miR-218-2*	ttgtgcttgatctaaccatgt
mmu-miR-122	tggagtgtgacaatggtgtttg
mmu-miR-125b-3p	acgggttaggctcttggga
mmu-miR-142-3p	tgtagtgtttcctactttatgga
mmu-miR-142-5p	gtcgcataaagtagaaagcactact
mmu-miR-144	gctggtctacagtatagatgatgtact
mmu-miR-451	aaaccgttaccattactgagtt
mmu-miR-486	tcctgtactgagctgcccc
mmu-miR-7a*	caacaaatcacagtctgccata
mmu6	gatacagagaagatttagcatgg

Morphological detection on the heart of pax-8 knockout mice

Hearts were harvested from E15.5 Pax-$8^{+/-}$ and Pax-$8^{-/-}$ mice and made for four-chamber heart sections for HE staining. Heart samples were fixed by perfusion with 10% formalin in 1× PBS and then were immersed in the same fixative solution for 72 hrs at room temperature. They were then dehydrated, and embedded in paraffin using standard histological procedures. Sections (4 μm) were treated by conventional HE staining. The hearts from newly born mice of the same groups were cut into thin sections for electron microscopy observation. About one cube millimetre size of the tissue was quickly isolated from the left ventricular wall and interventricular septum, fixed in 2.5% glutaraldehyde for 1 week. The electron microscope samples were post-fixed in 1% osmium tetroxide for 1 hr, and then embedded in epoxy resin for thin section transmission electron microscopy.

Cell culture

The H9C2 myocytes were obtained from the cell bank of the Chinese Academy of Sciences, Shanghai, China. The cells were cultured with DMEM (high glucose; Gibco BRL, Gaithersburg, MD, USA) medium containing 10% foetal bovine serum (FBS) (Gibco BRL) in a humidified atmosphere of 95% O_2, 5% CO_2 at 37°C in a CO_2 incubator. When the cells were grown to 90% confluence, they were then harvested by a brief exposure to 0.05% trypsin-EDTA (Gibco BRL) and passaged every 3 days.

Synthesis of miR-122 mimics

The positive-sense strand of miR-122 mimics (Sigma-Aldrich, St. Louis, MO, USA) was as follows: 5′-UGGAGUGUGACAAUGGUGUUUG-3′, and its antisense strand: 5′-AACACCAUUGUCACACUCCAUU-3′, having no homology with genome of rats. Different doses of FAM-NC miRNA/Lipofectamine™2000 (Invitrogen) were transfected into H9C2 (2-1) myocytes (blank control group, 2.5 μl/2.5 μl group, 5 μl/5 μl group, 7.5 μl/7.5 μl group). Transfection efficiency was detected by flow cytometry (BD, Valencio, CA, USA) 24 hrs later.

Transduction of miR-122

Single-cell suspension was prepared 24 hrs before transfection and cultured into six-well plate with the density of 1×10^5/well. The H9C2 (2-1) myocytes were transfected using LipofectamineTM2000 (Invitrogen) according to the manufacturer's instruction. They were divided into three groups, miR-122 group (experimental group), Negative Control (NC) miRNA group and Blank Control group. The miR-122 mimics were transfected into H9C2 (2-1) myocytes as experimental group. The microRNA synthesized randomly was transfected into H9C2 (2-1) myocytes as negative control group. The H9C2 myocytes were offered with routine culture medium with no miRNA as Blank Control group. Forward test was carried out after the cells were cultured at 37°C in an incubator containing 5% CO_2 for 24 or 48 hrs.

RNA extraction from H9C2 and real-time quantitative reverse transcriptase-polymerase chain reaction

Total RNAs were extracted through one-step method with Trizol (Invitrogen). The purity of total RNAs was detected by a spectrophotometer analyser (DU800) (Beckman, Miami, FL, USA) and its quality was detected by formaldehyde denaturation gel electrophoresis. Total 60 ng RNAs were obtained. The microRNA Isolation Kit (Ambion) was used to detach small molecular RNA less than 100nt, and miScript Reverse Transcription Kit (Qiagen) was adopted to synthesize cDNA through reverse transcription. At last, real-time quantitative PCR detection was carried out with ABI 7500 FAST real-time PCR. The PCR condition: 95°C 5 sec., 60°C 34 sec., 40 cycles. As an internal control, U6 primers were used for RNA template normalization. Fluorescent signals were normalized to an internal reference, and the threshold cycle (CT) was set within the exponential phase of the PCR. Sequence Detection system (SDS) 2.2.2 of Biosystems was used to analyse the data, and $^{\triangle\triangle}$CT was used to calculate relative-expression (RQ) of sample aim gene. The relative quantification of gene expression was analysed by the $2^{-\triangle\triangle CT}$ method [13] and was presented as fold over the control. The RQ = $2^{-\triangle\triangle CT}$ (CT was indicated to the cycles required by fluorescence signal intensity reaching to the threshold value in PCR amplification process.), $^{\triangle}CT_{sample} = CT_{sample} - CT\ U6_{sample}$, $^{\triangle}CT_{control} = CT_{control} - CT\ U6_{control}$, $^{\triangle\triangle}CT = {}^{\triangle}CT_{sample} - {}^{\triangle}CT_{control}$). The test was repeated three times.

Inhibition ratio was detected by CCK-8 assay

Single-cell suspension was prepared 24 hrs before transfection and cultured into a 96-well plate with the density of 7000/well. Twenty-four hours after transfection, the CCK-8 (Tong-ren Chemistry Institute of Japan) prepared solution was added, then incubated one hour at 37°C away from light. A_{450} was detected by ELISA Elx800 (Bio-Tex, Winooski, VT, USA) at last. Cell inhibitor ratio indicated that [(Blank ControlA_{450}–Experimental groupA_{450})/(Blank ControlA_{450}–Background ControlA_{450})]. Experimental group A_{450} and Blank ControlA_{450} indicated the absorbances of experimental group A_{450}, Negative ControlA_{450} or Blank ControlA_{450} at $\lambda = 405$ nm; Background Control A_{450} indicated the absorbances of 10% FBS + DMEM medium at $\lambda = 405$ nm.

Analysis of caspase-3 activity

Within 48 hrs, cells of each group were collected and protein was extracted. Two hundred micrograms of protein reacted with Caspase-3 background according to the instruction manual of Caspase-3 spectrophotometry Kit (Nanjing Kaiji Company, Nanjing, JiangSu, China) after protein concentration was detected by BCA assay with protein concentration determination kit (Pierce, Rockford, IL, USA). The absorbance A value at $\lambda = 405$ nm by ELISA ECX800 (Bio-TEX) was as experimental value. The specific Caspase-3 activity was calculated by the equation, OD (experimental group) − OD (background group): OD (experimental group) indicated the absorbance of interference group, Negative control group or blank control group at $\lambda = 405$ nm; OD (background) indicated the absorbance of the background containing 2× Reaction buffer 50 μl and Lysis buffer 50 μl at $\lambda = 405$ nm.

Cell apoptosis ratio was detected by AnnexinV/PI double dyeing with flow cytometry

Single-cell suspension was prepared and cultured into a six-well plate with the density of 1×10^5/hole. Forty-eight hours after transfection, cells of each group were collected, washed with PBS once, centrifugated (discarded supernatant), resuspended with 200 μl binding buffer, added with 5 μl of AnnexinV-FITC, 10 μl of PI and incubated for 15 min. away from light, detected with flow cytometry (BD), and at last, the data were analysed with the software of MULTCYCLE.

Synthesis of Pax-8 siRNA and miR-122 inhibitor

As previously mentioned, transduction of miR-122 resulted in the lower rates of cell proliferation, increased Caspase-3 activity, and higher apoptosis in primary cultures of H9C2 myocytes. To further study the function of miR-122 in the pathogenesis of congenital heart disease, especially in the mechanism of VSD, miR-122 inhibitor was transfected 24 hrs before Pax-8 siRNA was transfected into H9C2 cells to induce apoptosis. Then we observed whether miR-122 inhibitor could protect H9C2 cells from apoptosis. The positive-sense strand of Pax-8 siRNA (Sigma-Aldrich) was as follows: 5′-GGAAGUGAGUAUU CUGGCATT-3′, and its antisense strand: 5′-UGCCAGAAUACUCACUUCC TG-3′, The sequence of miR-122 inhibitor (Sigma-Aldrich) was as follows: 5′-CAAACACCAUUGUCACACUCCA-3′, no homology with genome of rats.

Transduction of Pax-8 siRNA and miR-122 inhibitor

Single-cell suspension was prepared 24 hrs before transfection and cultured into a six-well plate with the density of 1×10^5/well. The H9C2 (2-1) myocytes were transfected using LipofectamineTM2000 (Invitrogen) according to the manufacturer's instruction. It was divided into four groups, Pax-8 siRNA + miR-122 inhibitor group (experimental group), Pax-8 siRNA group (apoptosis induction group), Negative Control (NC) miRNA group and Blank Control group. Pax-8 siRNA was transfected into H9C2 (2-1) myocytes as apoptosis induction group. The miR-122 inhibitor was transfected 24 hrs before Pax-8 siRNA was transfected into H9C2 (2-1) myocytes. The miRNA, synthesized randomly, was transfected into H9C2 (2-1) myocytes as negative control group. The H9C2 myocytes were offered with routine culture medium with no miRNA as Blank Control group. Forward test was carried out after these cells were cultured at 37°C in incubator containing 5% CO_2 for 24 or 48 hrs.

Statistics

The data were analysed with the software of SPSS 17.0. All experiments were repeated three times and presented as mean ± SE. The multiple groups were analysed by one-way ANOVA followed by Tukey's *post hoc* comparisons. Differences were considered statistically significant at $P < 0.05$.

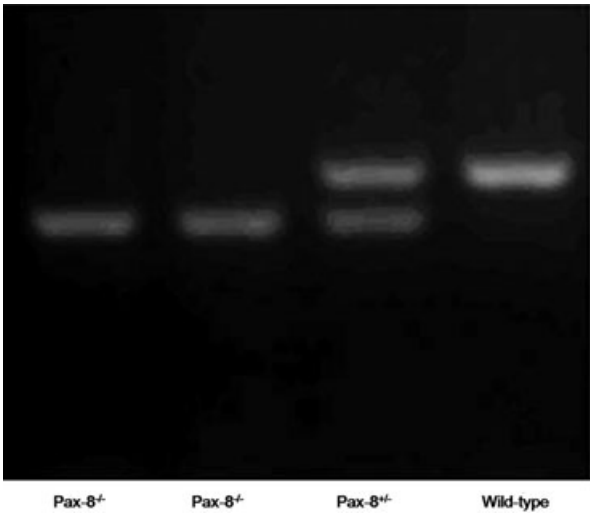

Fig. 1 Identification of pax-8 knockout mouse model. The PCR genotyping showed that Pax-$8^{-/-}$ had a single band of about 370 bp. The wild-type had a single band of about 390 bp. Pax-$8^{+/-}$ had two bands of 390 and 370 bp.

Result

miRNAs differentially expressed in Pax-8 knockout mice

The PCR genotyping shows that Pax-$8^{-/-}$ had a single band of about 370 bp. The wild-type had a single band of about 390 bp. Pax-$8^{+/-}$ had two bands of 390 and 370 bp (Fig. 1).

We further studied the expression of 443 known miRNAs in Pax-$8^{-/-}$ (test group) and Pax-$8^{+/-}$ (control group) using the miRNAs microarray. The change in the level of miRNA expression over twofold was considered as positive. We found that there were significant reductions in expression of 2 miRNAs (miR-148a*, miR-218-2*), whereas there were eight miRNAs (miR-122, miR-125b-3p, miR-142-3p, miR-142-5p, miR-144, miR-451, miR-486, miR-7a) up-regulated in test group (Table 2). The 10 differential expressed miRNAs were confirmed by real-time PCR. The results showed that eight of them were up-regulated (miR-451, 8.98-fold, miR-142-3p 7.77-fold, miR-144 2.80-fold, miR-7a* 1.99-fold, miR-122, 1.92-fold, miR-142-5p, 1.85-fold, miR-148a*, 1.59-fold, miR-486, 1.21-fold) and in miR-125-3p there was 0.56-fold reduction. MiR-218-2* was failed to detect by PCR because of low lead content of samples (Table 3).

Developmental defects occurring in the hearts of Pax-8 KO mice

Ventricular septum defect (VSD) was found by H&E staining in the hearts of Pax-$8^{-/-}$ mice (Fig. 2). By electron microscopy, we observed that Pax-$8^{-/-}$ mice had fairly organized structures of the myofilament and sarcomere in the left ventricular wall and interventricular septum. However, there were a large number of myocardial apoptosis cells with cell shrink, cytoplasmic vacuoles, marked increases of the number of mitochondria and decreases in volume, chromatin concentration and side shifts and formations of apoptotic bodies. The H&E staining of Pax-$8^{+/-}$ mice hearts showed no significant change in the structure. The electron microscopy observation of Pax-$8^{+/-}$ mice hearts showed no significant expansion of sarcoplasmic reticulum, the moderate myocardial apoptosis cells, and no obvious abnormalities in size and amount of the mitochondria was found (Fig. 2, more details were showed at *Int J Cardiol.* 2012; 154: 43–51).

Table 2 miRNAs differential expression between Pax-$8^{-/-}$ and Pax-$8^{+/-}$ by microRNA microarray

	miRNA	Fold change
Up-regulated	mmu-miR-122	3.13
	mmu-miR-125b-3p	2.91
	mmu-miR-142-3p	2.90
	mmu-miR-142-5p	3.00
	mmu-miR-144	3.92
	mmu-miR-451	3.41
	mmu-miR-486	2.11
	mmu-miR-7a*	2.31
Down-regulated	mmu-miR-148a*	0.47
	mmu-miR-218-2*	0.002

Increased apoptosis of H9c2 myocytes by transduction of miR122

To further study the function of miR-122 in the pathogenesis of congenital heart disease, especially in the mechanism of VSD, H9C2 cells were transfected with the appropriate miR-122 mimics. Transfection efficiency was detected by flow cytometry 24 hrs after different doses of FAM-NC miRNA/LipofectamineTM2000 were transfected into H9C2 (2-1) myocytes. Transfection efficiencies of different groups were shown. (A) Blank Control was 0.1%; (B) 2.5/2.5 μl group was 81.0%; (C) 5/5 μl group was 96.6%; (D) 7.5/7.5 μl group was 98.7%. Considering transfection efficiency and toxicity derived from high concentration of miRNA/LipofectamineTM2000, miRNA 5 μl/Lipofectamine TM2000 was chosen as a transfection condition. High concentration of miRNA/LipofectamineTM2000 (C and D group) could cause cell necrosis which could interfere with experimental results (Fig. 3).

miR-122 transduction induces CCK-8 and caspase-3

The result of miR-122 quantitative reverse transcriptase-polymerase chain reaction (qRT-PCR) indicated that the level of miR-122

Table 3 miRNAs differential expression by real-time PCR analysis

miRNA	Pax-8$^{-/-}$	Pax-8$^{+/-}$	Fold change	*t*	*P*
mmu-miR-125b-3p	0.0110 ± 0.001	0.0195 ± 0.0019	0.56	6.747	0.003
mmu-miR-7a*	0.0015 ± 0.0002	0.0008 ± 0.0002	1.99	4.884	0.008
mmu-miR-142-3p	0.0214 ± 0.0030	0.0028 ± 0.0008	7.77	10.393	0.000
mmu-miR-122	0.0066 ± 0.0008	0.0034 ± 0.0003	1.92	6.253	0.003
mmu-miR-142-5p	0.0009 ± 0.0002	0.0005 ± 0.0002	1.85	3.526	0.024
mmu-miR-144	0.0046 ± 0.0001	0.0017 ± 0.0004	2.80	12.224	0.000
mmu-miR-451	6.2110 ± 0.6564	0.6953 ± 0.1116	8.98	14.348	0.000
mmu-miR-486	1.8601 ± 0.5207	1.4806 ± 0.0259	1.21	1.261	0.276
mmu-miR-148a*	0.3294 ± 0.0167	0.2096 ± 0.0346	1.59	5.406	0.006

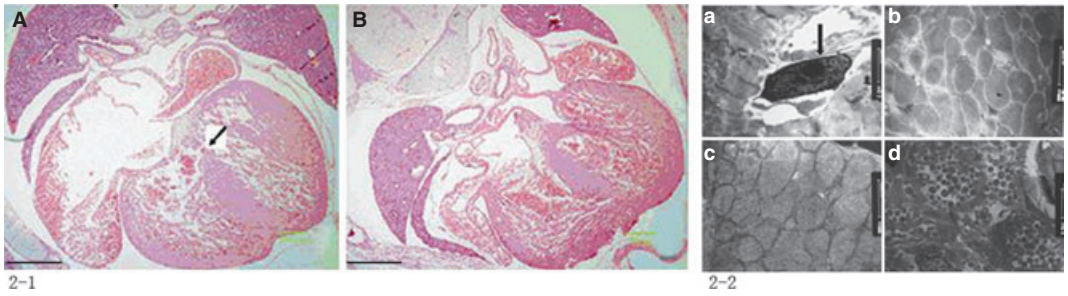

Fig. 2 (2-1) HE staining observation in E15.5 Pax-8 KO mice heart. (**A**) Hearts were isolated from Pax-8$^{-/-}$ mice whose ventricular septum defect was indicated by an arrow (×400). (**B**) Hearts were isolated from Pax-8$^{+/-}$ whose morphology was essentially normal (×400). The VSD was found by H&E staining in the hearts of Pax-8$^{-/-}$ mice. Scale bars = 1mm (**A**, **B**). (2-2) Electron microscope observation in Pax-8 KO mice heart. (**a**) Apoptosis cell in the left ventricular wall of Pax-8$^{-/-}$ mice, 6200×. (**b**) Mitochondria in the left ventricular wall of Pax-8$^{-/-}$ mice showed increase in the amount and decrease in the size, 17,500×. (**c**) Mitochondria in the left ventricular wall of Pax-8$^{+/-}$ mice showed no significant change in both amount and size, 17,500×. (**d**) Full view of the mitochondria in the left ventricular wall of Pax-8$^{-/-}$ mice, 3700×. The black-colour cell in the centre indicated with an arrow was considered apoptosis, with cell shrink, cytoplasmic vacuoles, marked increases of the number of mitochondria and decreases in volume, chromatin concentration and side shifts and formations of apoptotic bodies.

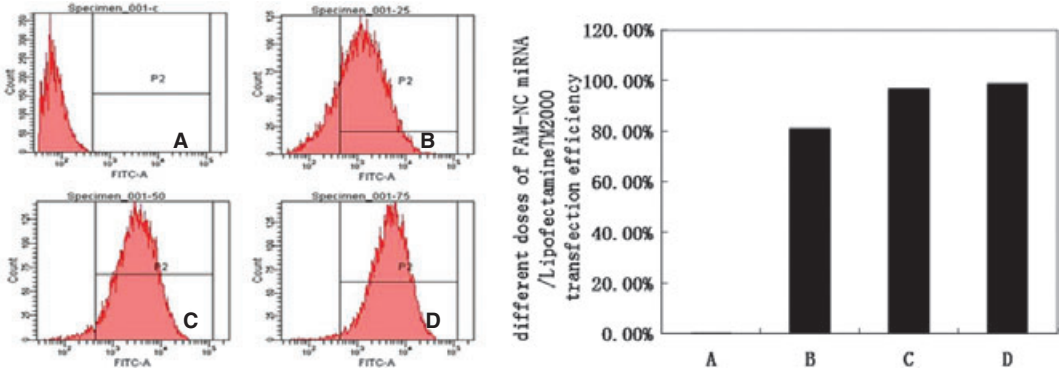

Fig. 3 Different doses of FAM-NC miRNA/LipofectamineTM2000 transfection efficiency to H9C2 cells after 24 hrs by flow cytometer. Right is the corresponding column. (**A**) Blank control group 0.1%; (**B**) 2.5 μl/2.5 μl group 81.0%; (**C**) 5 μl/5 μl group 96.6%; (**D**) 7.5 μl/7.5 μl group 98.7%. Transfection efficiencies of the different groups were shown that Blank Control was 0.1% (**A**), 2.5 μl/2.5 μl group was 81.0% (**B**), 5 μl/5 μl group was 96.6% (**C**), 7.5 μl/7.5 μl group was 98.7% (**D**).

expression in H9C2 (2-1) myocytes transfected into miR-122 mimics (108.90 ± 1.90) was obviously higher than that of negative control miRNA group (0.41 ± 0.02) and blank control group (1.00 ± 0.00) ($P < 0.01$) while the latter two groups had no significant statistical difference ($P > 0.05$) (Fig. 4-1).

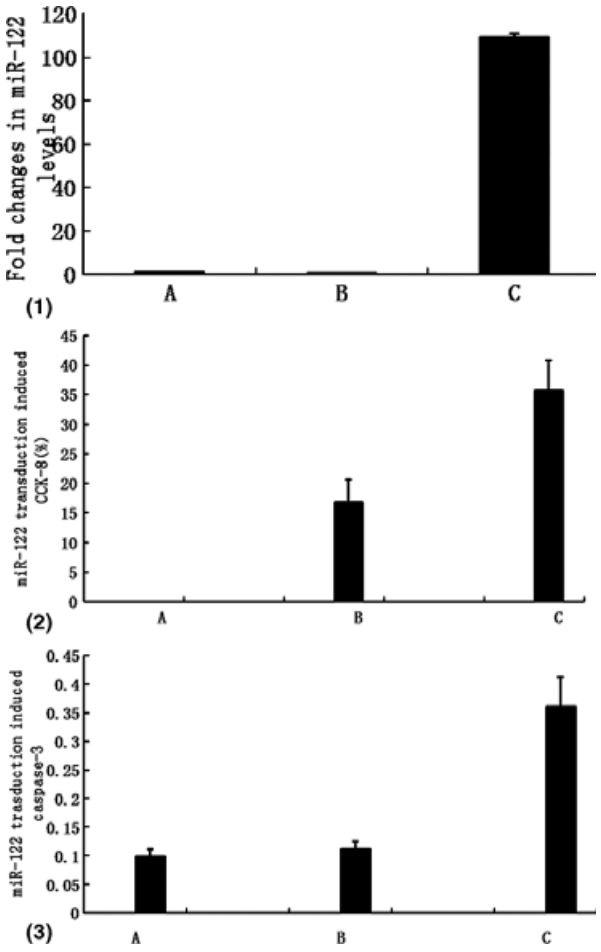

Fig. 4 (4-1) Result of miR-122 qRT-PCR. (**A**) Blank control group; (**B**) Negative control miRNA group; (**C**) miR-122 group miR-122 expression in miR-122 mimics group (108.90 ± 1.90) was obviously higher than that of NC miRNA group (0.41 ± 0.02) and Blank Control group (1.00 ± 0.00) ($P < 0.01$) while the latter two groups had no significant statistical difference ($P > 0.05$). (4-2) miR-122 transduction induced CCK-8. (**A**) Blank control group; (**B**) Negative control miRNA group; (**C**) miR-122 group. The inhibition index was higher in the cells of the miR-122 group (35.64 ± 3.82%) than that of the negative control miRNA group (16.77 ± 5.06%) ($P < 0.01$). (4-3) miR-122 transduction induced caspase-3. (**A**) Blank control group; (**B**) Negative control miRNA group; (**C**) miR-122 group. The caspase-3 activity of miR-122 group (0.361 ± 0.051) was obviously higher than that of negative control miRNA group (0.112 ± 0.014) and blank control group (0.099 ± 0.012) ($P < 0.01$), while the latter two group had no significant statistical difference ($P > 0.05$).

The role of the miR-122 in the mechanism of VSD was determined by examining its apoptosis and proliferation abilities. The inhibition index was higher in the cells of the miR-122 group (35.64 ± 3.82%) than that of the negative control miRNA group (16.77 ± 5.06%) ($P < 0.01$) (Fig. 4-2). Pairwise comparison among three groups, caspase-3 activity of miR-122 group (0.361 ± 0.051) was obviously higher than that of negative control miRNA group (0.112 ± 0.014) and blank control group (0.099 ± 0.012) ($P < 0.01$), while the latter two groups had no significant statistical difference ($P > 0.05$) (Fig. 4-3).

Increased apoptosis in H9C2 cells with miR-122 transduction

We observed that 24 hrs after transduction, the index of apoptosis of miR-122 transduced H9C2 cells (13.00 ± 0.76%) was obviously higher than that of the negative control miRNA (5.13 ± 1.25%) and blank control cells(4.500 ± 1.179%) ($P < 0.01$), while the latter two groups had no significant statistical difference ($P > 0.05$) (Fig. 5A1–C1). Forty-eight hours after transduction, pairwise comparison among three groups, cell apoptosis ratio of miR-122 group (20.033 ± 0.416%) was obviously higher than that of negative control miRNA group (6.233 ± 0.306%) and blank control group (5.467 ± 0.764%) ($P < 0.01$) while the latter two groups had no significant statistical difference ($P > 0.05$) (Fig. 5A2–C2). The phenomenon showed its time-dependent manner. Cell apoptosis ratio of miR-122 group (20.033 ± 0.416%) was higher 48 hrs after transduction.

Fold changes in Pax-8 and miR-122 levels after Pax-8 siRNA and miR-122 inhibitor transfection

As above mentioned, transduction of miR-122 resulted in the lower rates of cell proliferation, increased Caspase-3 activity and higher apoptosis in primary cultures of H9C2 myocytes. To further study the function of miR-122 in the pathogenesis of congenital heart disease, especially in the mechanism of VSD, miR-122 inhibitor was transfected 24 hrs before Pax-8 siRNA was transfected into H9C2 cells to induce apoptosis. Then we observed whether or not miR-122 inhibitor could protect H9C2 cell from apoptosis. The result of Pax-8 qRT-PCR indicated that the level of Pax-8 expression in H9C2 (2-1) myocytes transduced with Pax-8 siRNA (0.055 ± 0.005) and Pax-8 siRNA + miR-122 inhibitor (0.060 ± 0.003) was obviously lower than that of the negative control miRNA group (0.968 ± 0.071) and blank control group (1.000 ± 0.000) ($P < 0.01$), while the previous and latter two groups had no significant statistical difference ($P > 0.05$) (Fig. 6-1). The result of miR-122 qRT-PCR indicated that the level of miR-122 expression in H9C2 (2-1) myocytes transduced with Pax-8 siRNA + miR-122 inhibitor (0.069 ± 0.003) was obviously lower than that of Pax-8 siRNA group (1.006 ± 0.071), negative control miRNA group (0.964 ± 0.081) and blank control group (1.000 ± 0.000) ($P < 0.01$), while the latter three groups had no significant statistical difference ($P > 0.05$) (Fig. 6-2).

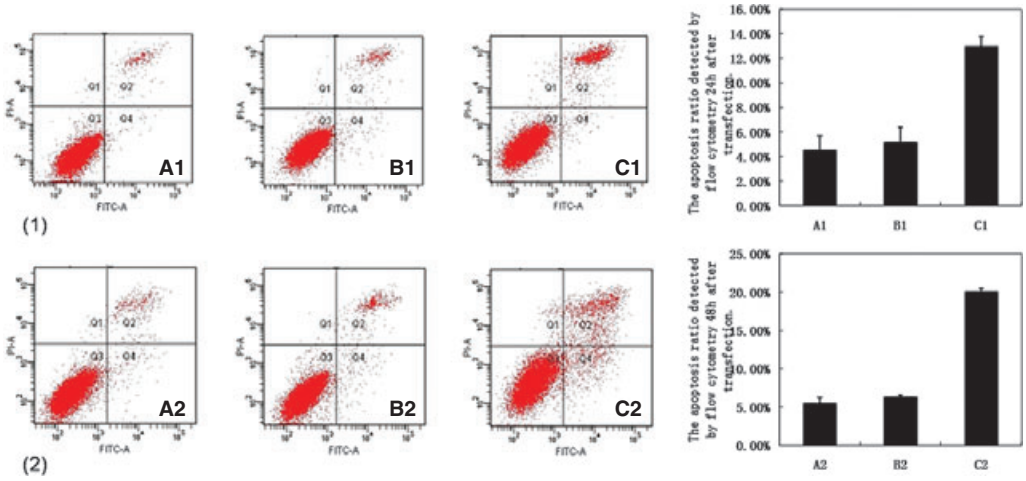

Fig. 5 The apoptosis ratio detected by flow cytometry 24 and 48 hrs after transduction. Right is the corresponding column. (**A1**) Blank control group (24 hrs); (**B1**) Negative control miRNA group (24 hrs); (**C1**) miR-122 group (24 hrs). (**A2**) Blank control group (48 hrs); (**B2**) Negative control miRNA group (48 hrs); (**C2**) miR-122 group (48 hrs). Twenty-four hours after transduction, the index of apoptosis of miR-122 transduced H9C2 cells (13.00 ± 0.76%) was obviously higher than that of the negative control miRNA (5.13 ± 1.25%) and blank control cells (4.500 ± 1.179%) ($P < 0.01$), while the latter two groups had no significant statistical difference ($P > 0.05$). Forty-eight hours after transduction, pairwise comparison among three groups, cell apoptosis ratio of miR-122 group (20.033 ± 0.416%) was obviously higher than that of negative control miRNA group (6.233 ± 0.306%) and blank control group (5.467 ± 0.764%) ($P < 0.01$) while the latter two group had no significant statistical difference ($P > 0.05$).

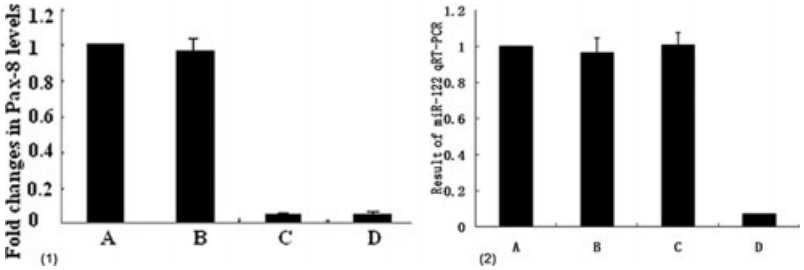

Fig. 6 (6-1) Result of Pax-8 qRT-PCR. (**A**) Blank control group; (**B**) Negative control miRNA group; (**C**) Pax-8 siRNA group; (**D**) Pax-8 siRNA + miR-122 inhibitor group. Pax-8 expression in Pax-8 siRNA group (0.055 ± 0.005) and Pax-8 siRNA + miR-122 inhibitor group (0.060 ± 0.003) was obviously lower than that of negative control miRNA group (0.968 ± 0.071)and blank control group (1.000 ± 0.000) ($P < 0.01$) while the previous and latter two groups had no significant statistical difference ($P > 0.05$). (6-2) Result of miR-122 qRT-PCR. (**A**) Blank control group; (**B**) Negative control miRNA group; (**C**) Pax-8 siRNA group; (**D**) Pax-8 siRNA + miR-122 inhibitor group. The miR-122 expression in Pax-8 siRNA + miR-122 inhibitor group (0.069 ± 0.003) was obviously lower than that of Pax-8 siRNA group (1.006 ± 0.071), negative control miRNA group (0.964 ± 0.081) and blank control group (1.000 ± 0.000) ($P < 0.01$) while the latter three groups had no significant statistical difference ($P > 0.05$).

miR-122 inhibitor transduction depresses CCK-8 and caspase-3

The role of the miR-122 in the mechanism of VSD was determined by examining its apoptosis and proliferation ability. As above mentioned, miR-122 transduction increased CCK-8 and caspase-3. While the inhibition index was higher in the cells of Pax-8 siRNA group (31.49 ± 3.16%) than that of negative control group (4.08 ± 4.46%) ($P < 0.01$), and the inhibition index was lower in the cells of Pax-8 siRNA + miR-122 inhibitor group (17.69 ± 2.33%) than that of Pax-8 siRNA group (31.49 ± 3.16%) ($P < 0.01$) (Fig. 7-1). Pairwise comparison among four groups, Caspase-3 activity of Pax-8 siRNA group (0.569 ± 0.023) was obviously higher than that of negative control group (0.261 ± 0.023) and blank control group (0.236 ± 0.025) ($P < 0.01$) while the latter two groups had no significant statistical differences ($P > 0.05$), and Caspase-3 activity of Pax-8 siRNA + miR-122 inhibitor group (0.426 ± 0.033) was obviously lower than that of the Pax-8 siRNA group (0.569 ± 0.023) ($P < 0.01$) (Fig. 7-2).

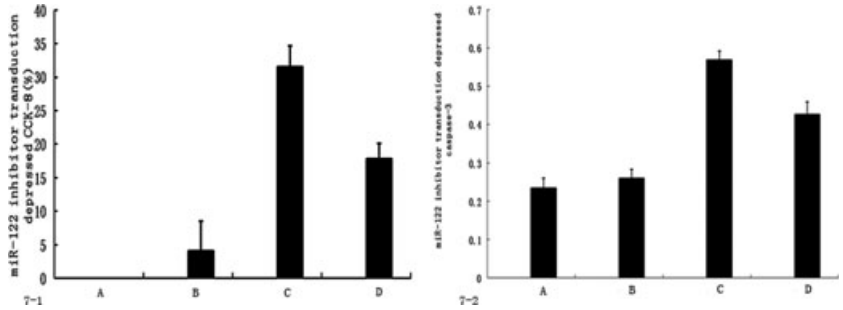

Fig. 7 (7-1) miR-122 inhibitor transduction depressed CCK-8. (**A**) Blank control group; (**B**) Negative control miRNA group; (**C**) Pax-8 siRNA group; (**D**) Pax-8 siRNA + miR-122 inhibitor group. The inhibition index was higher in the cells of Pax-8 siRNA group (31.49 ± 3.16%) than that of negative control group (4.08 ± 4.46%) ($P < 0.01$), and the inhibition index was lower in the cells of Pax-8 siRNA + miR-122 inhibitor group (17.69 ± 2.33%) than that of Pax-8 siRNA group (31.49 ± 3.16%) ($P < 0.01$). (7-2) miR-122 inhibitor transduction depressed caspase-3. (**A**) Blank control group; (**B**) Negative control miRNA group; (**C**) Pax-8 siRNA group; (**D**) Pax-8 siRNA + miR-122 inhibitor group. The caspase-3 activity of Pax-8 siRNA group (0.569 ± 0.023) was obviously higher than that of negative control group (0.261 ± 0.023) and blank control group (0.236 ± 0.025) ($P < 0.01$) while the latter two groups had no significant statistical differences ($P > 0.05$), and Caspase-3 activity of Pax-8 siRNA + miR-122 inhibitor group (0.426 ± 0.033) was obviously lower than that of the Pax-8 siRNA group (0.569 ± 0.023) ($P < 0.01$).

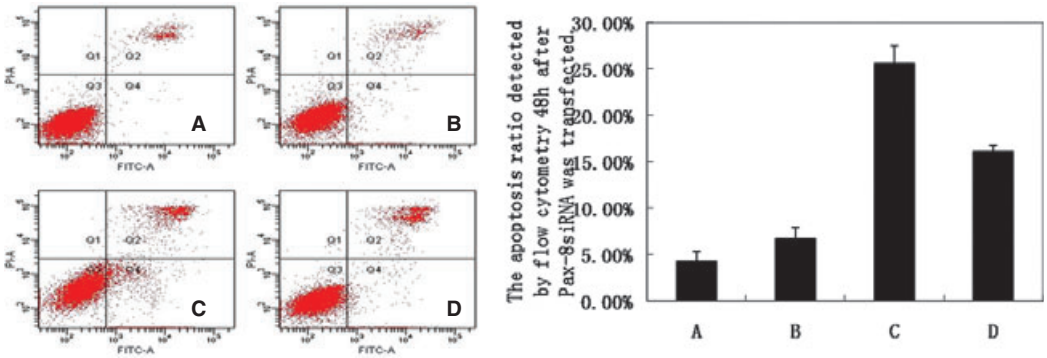

Fig. 8 The apoptosis ratio detected by flow cytometry 48 hrs after Pax-8 siRNA was transfected. Right is the corresponding column. (**A**) Blank control group; (**B**) Negative control miRNA group; (**C**) Pax-8 siRNA group; (**D**) Pax-8 siRNA + miR-122 inhibitor group. Forty-eight hours after transduction, the index of apoptosis of Pax-8 siRNA transduced H9c2 cells (25.57 ± 1.88%) was obviously higher than that of negative control miRNA (6.70 ± 1.23%) and blank control cells (4.33 ± 1.00%) ($P < 0.01$) while the latter two groups had no significant statistical difference ($P > 0.05$) and the index of apoptosis of Pax-8 siRNA + miR-122 inhibitor transduced H9c2 cells (16.10 ± 0.70%) was obviously lower than that of Pax-8 siRNA group (25.57 ± 1.88%) ($P < 0.01$).

Increased apoptosis in H9C2 cells with Pax-8 siRNA transduction, while decreasing apoptosis when they were transduced with miR-122 inhibitor 24 hrs before Pax-8 siRNA transduction

We observed that 48 hrs after transduction, the index of apoptosis of Pax-8 siRNA transduced H9c2 cells (25.57 ± 1.88%) was obviously higher than that of negative control miRNA (6.70 ± 1.23%) and blank control cells (4.33 ± 1.00%) ($P < 0.01$) while the latter two groups had no significant statistical difference ($P > 0.05$) and the index of apoptosis of Pax-8 siRNA + miR-122 inhibitor transduced H9c2 cells (16.10 ± 0.70%) was obviously lower than that of Pax-8 siRNA group (25.57 ± 1.88%) ($P < 0.01$) (Fig. 8).

Discussion

Many miRNAs have been found in vertebrates. Their functions in the ontogenetic process, especially in the process of cell development are deeply investigated [14, 15]. The microRNAs also play an important role in the process of myocardial injury and apoptosis. *Pax* belongs to an important gene family related to development, and Pax protein is an important transcription regulator that plays an important role in the differentiation of tissues and organs during embryonic development. Pax-8 is one transcription factor of the family of mammals Pax protein. Pax-8 gene expression has tissue specificity. Pax-8 knockout mice develop thyroid dysplasia and thyroxine descent [16]. In current studies, significant structural abnormalities of the heart of Pax-8 knockout mice including ventricular septum defect are found. A large

number of myocardial apoptosis cells in the left ventricular wall and interventricular septum are further confirmed by electron microscopy. The volume of the mitochondria within cells is reduced and the quantity is increased.

In microarray studies, 10 miRNAs were differentially expressed in significance between pax-$8^{+/-}$ and pax-$8^{-/-}$ mice hearts. The level of expression of eight miRNAs was significantly up-regulated in pax-$8^{-/-}$ by 1.21- to 8.98-fold (miR-451, 8.98-fold, miR-142-3p, 7.77-fold, miR-144, 2.79-fold, miR-7a, 1.98-fold, miR-122, 1.92-fold, miR-142-5p, 1.85-fold, miR-148, 1.59-fold, miR-486, 1.21-fold). The level of expression of miR-125-3p was reduced by 0.56-fold. The miR-218-2 was not detected by RT-PCR. And miR-142-3p was found probably closely related to the haemopoietic system disease [17], miR-451 is being revealed to participate in the late stages of erythropoiesis [18] and closely related to the resistance of cancer cell to a broad range of chemotherapeutics [19]. The role of both in the heart development has not yet been reported. In this study miR-122 mimics were transfected into H9C2 (2-1) myocardial cells of rat to up-regulate miR-122 expression. In up-regulated miR-122 group, myocardial apoptosis was increased while proliferation inhibited, indicating that miR-122 might promote myocardial cell apoptosis. As miR-122 may promote myocardial cell apoptosis, then what's the role of miR-122 inhibitor in myocardial cell apoptosis. Therefore, in the following experiment, the H9C2 (2-1) myocardial cells transfected with Pax-8 siRNA were as an apoptotic model. Then miR-122 inhibitor was transfected into H9C2 (2-1) myocardial cells 24 hrs before Pax-8 siRNA was transfected. At last, we observed whether miR-122 inhibitor had protective role in cell apoptosis. We found that the expression of Pax-8 in H9C2 (2-1) myocardia cells trasfected with Pax-8 siRNA was down-regulated, which caused increased myocardial apoptosis and inhibited proliferation. However, when H9C2 (2-1) myocardia cells were transfected with miR-122 inhibitor 24 hrs before Pax-8 siRNA, we found cell apoptosis decreasing and proliferation increasing compared with those only transfected with Pax-8 siRNA. So we infer an individual miRNA such as miR-122 may be a new target for the therapy of VSD. Modulating the expression of a single microRNA can, in principle, influence an entire gene network and thereby modify complex disease phenotypes. It has been reported that a kind of miRNA antagonist rectifying fault signal transduction pathway had the potency of target prevention and therapy.

However, in our research there also exists defects. In Pax-8 knockout mice, Pax-8 gene was silent completely, and we found 10 miRNAs were differentially expressed, among which miR-122 was up-regulated 1.92 fold. However, RNA interference was often used to partly silence gene expression. When the H9C2 (2-1) myocardial cells transfected with Pax-8siRNA were as apoptotic model to study whether miR-122 inhibitor had protective role in cell apoptosis, Pax-8 gene was silent partly. Besides, the fold that miR-122 up-regulated in Pax-8 knockout mice was only 1.92, so when Pax-8 was down-regulated with siRNA, the level of the miR-122 expression was not increased significantly.

Our research showed that the apoptosis in the Pax-8 siRNA + miR122 inhibitor transduced H9C2 cells was still high (Fig. 8): 16% (in D) *versus* 6.7% (in B). This suggests that miR-122 alone is not sufficient to ablate the apoptotic events induced by down-regulation of Pax-8. That is to say that other genes may participate in apoptotic events induced by down-regulation of Pax-8. We have used gene chip to identify down-stream genes of Pax-8.

As to the potential target genes of the 10 miRNAs, we have used miRNAs target prediction software (pictar, targetscan, miRBase) to screen the target genes. HAND2 which is the potential target gene of miR-122 is a basic helix-loop-helix (bHLH) transcription factor that plays an essential role in cardiac morphogenesis. In HAND2 mutant embryos, the right ventricle (RV) forms but apoptosis undergoes [20], suggesting that Hand2 may be required for survival of the cardiomyocytes. Loss of HAND2 in the natural cytotoxic lineage leads to misalignment of the outflow tract and aortic arch arteries. HAND2 related defects include pulmonary stenosis, interrupted aortic artery, retro-oesophageal right subclavian artery and ventricular septum defect [21]. Disruption of HAND2 severely impairs development of the right ventricle, outflow tract and aortic arch arteries, indicating that HAND2 is indispensable for the formation of the superior elements of the developing heart [22]. In patients with right ventricular hypertrophy (*e.g.* tetralogy of Fallot), the level of HAND2 mRNA expression is increased [23]. The investigation of HAND2 mutations in 131 Chinese congenial heart disease (CHD) children indicates that HAND2 would be a potential candidate gene of some kinds of CHD [24]. How miR-122 regulates HAND2 gene expression needs further study.

The potential target genes of miR-144 include Apaf-1, Caspase-3, MAP3K4, LGR4 and so on. Apoptotic protease activating factor-1 (Apaf-1) binds to cytochrome *c* (Cyt *c*) released from cells to form complexes called apoptosomes, and then bind to and cleave caspase-9 precursors, which creates an expanding cascade of proteolytic activity and causes apoptosis. This is one of the classic pathways of apoptosis. However, Dmitriy Ovcharenko *et al.* [25] predicted that miR-144 directly targeted caspase-3 to achieve anti-apoptosis effect. The mitogen-activated protein kinase kinase kinase 4 (MAP3K4) has been identified as a crucial anti-apoptotic element required for normal development of mouse embryo by regulation of the MKK3/p38/MAPKAPK-2 pathway [26], hence miR-144 may also target MAP3K4 to induce apoptosis. On account of these two aspects, we could presume that miR-144 plays different roles at different time points: it may be mainly to induce apoptosis at the stage of embryonic development and inversely mainly inhibit apoptosis in the adult. One of the potential target genes LGR4 is widely distributed in the embryo and adult, Mazerbourg *et al.* [27] indicated that LGR4 was closely related to the process of embryonic development in LGR4 knockout mouse model. On the other hand, after the prediction of the target genes of miR-125-3p, the LBH gene related to heart development has aroused our interest. Briegel *et al.* [28] have used transgenic technology to make LBH excessive expression, which leads to severe defects in morphology and function of heart, such as left ventricular hypertrophy, ventricular septum defect and so on, and this finding is similar to our study on Pax-8 knockout mouse, hence we can presume miR-125-3p could be involved in the abnormal heart development of pax-8 knockout mouse embryo by targeting LBH.

In summary, to assess the involvement of miRNA in the pathogenesis of congenital heart disease, especially in the mechanism of VSD development, we analysed differential miRNA expression in Pax-8 gene knockout mice. We found that miR-122 was up-regulated sig-

nificantly. The role of miR-122 in apoptosis of myocardial cells was confirmed by using miR-122 mimics and miR-122 inhibitor transfected into H9C2 (2-1) myocytes respectively. Transduction of miR-122 mimics resulted in the lower rates of cell proliferation, increased Caspase-3 activity and higher apoptosis in primary cultures of H9C2 myocytes, and transduction of Pax-8 siRNA into H9C2 (2-1) myocytes resulted lower expression of Pax-8, correspondingly causing increased caspase-3 activity, higher apoptosis and decreased cell proliferation. However, when H9C2 (2-1) myocardia cells were transfected with miR-122 inhibitor 24 hrs before Pax-8 siRNA, we found cell apoptosis decreasing and proliferation increasing compared with those only transfected with Pax-8 siRNA.

Acknowledgements

This work was supported by the grants from the National Natural Science Foundation of China (30571050) and Zhejiang Province Natural Science Foundation (Y2110112). We thank professor Peter Gruss and Professor Ahmed Mansouri for their support and help, especially for providing experimental animals. We also thank professor Yong-Jian Geng for technical help.

Conflict of interest

The authors confirm that there are no conflicts of interest.

References

1. **Choi YJ, Lin CP, Ho JJ, *et al.*** miR-34 miRNAs provide a barrier for somatic cell reprogramming. *Nat Cell Biol.* 2011; 13: 1353–60.
2. **Cesana M, Cacchiarelli D, Legnini I, *et al.*** A long noncoding RNA controls muscle differentiation by functioning as a competing endogenous RNA. *Cell.* 2011; 147: 358–69.
3. **Mukhopadhyay P, Das S, Gorbunov N, *et al.*** Modulation of miroRNA 20b with resveratrol and longevinex is linked with their potent anti-angiogenic action in the ischaemic myocardium and synergestic effects of resveratrol and γ-tocotrienol. *J Cell Mol Med.* 2011, Doi: 10.1111/j.1582-4934.2011.01480.x.
4. **Wu LG, Fan JH, Belasco JG.** MicroRNAs direct rapid deadenylation of mRNA. *Proc Natl Acad Sci USA.* 2006; 103: 4034–9.
5. **Formosa A, Piro MC, Docimo R, *et al.*** Salivary miRNAome profiling uncovers epithelial and proliferative miRNAs with differential expression across dentition stages. *Cell Cycle.* 2011; 10: 3359–68.
6. **Bae S, Lee EM, Cha HJ, *et al.*** Resveratrol alters microRNA expression profiles in A549 human non-small cell lung cancer cells. *Mol Cells.* 2011; 32: 243–9.
7. **Truscott M, Islam AB, Lopez-Bigas N, Frolov MV.** mir-11 limits the proapoptotic function of its host gene, dE2f1. *Genes Dev.* 2011; 25: 1820–34.
8. **Zhao Y, Samal E, Srivastava D.** Serum response factor regulates a muscle-specific microRNA that targets Hand2 during cardiogenesis. *Nature.* 2005; 436: 214–20.
9. **Fiedler J, Jazbutyte V, Kirchmaier BC, *et al.*** MicroRNA-24 regulates vascularity after myocardial infarction. *Circulation.* 2011; 124: 720–30.
10. **Hoffman JI, Kaplan S.** The incidence of congenital heart disease. *J Am Coll Cardiol.* 2002; 39: 1890–900.
11. **Nemer M.** Genetic insights into normal and abnormal heart development. *Cardiovasc Pathol.* 2008; 17: 48–54.
12. **Yang D, Lai D, Huang X, *et al.*** The defects in development and apoptosis of cardiomyocytes in mice lacking the transcriptional factor Pax-8. *Int J Cardiol.* 2012; 154: 43–51.
13. **Livak KJ, Schmittgen TD.** Analysis of relative gene expression data using real-time quantitative PCR and the 2(-Delta Delta C (T)) Method. *Methods.* 2001; 25: 402–8.
14. **Yang F, Zhang L, Wang F, *et al.*** Modulation of the unfolded protein response is the core of microRNA-122-involved sensitivity to chemotherapy in hepatocellular carcinoma. *Neoplasia.* 2011; 13: 590–600.
15. **Yin J, Tang HF, Xiang Q, *et al.*** MiR-122 increases sensitivity of drug-resistant BEL-7402/5-FU cells to 5-fluorouracil *via* down-regulation of bcl-2 family proteins. *Pharmazie.* 2011; 66: 975–81.
16. **Mansouri A, Chowdhury K, Gruss P.** Follicular cells of the thyroid gland require pax-8 gene function. *Nat Genet.* 1998; 19: 87–90.
17. **Ramkissoon SH, Mainwaring LA, Ogasawara Y, *et al.*** Hematopoietic-specific microRNA expression in human cells. *Leuk Res.* 2006; 30: 643–47.
18. **Bruchova H, Yoon D, Agarwal AM, *et al.*** Regulated expression of microRNAs in normal and polycythemia vera erythropoiesis. *Exp Hematol.* 2007; 35: 1657–67.
19. **Zhu H, Wu H, Liu X, *et al.*** Role of microRNA miR-27a and miR-451 in the regulation of MDR1/P-glycoprotein expression in human cancer cells. *Biochem Pharmacol.* 2008; 76: 582–8.
20. **Yamagishi H, Yamagishi C, Nakagawa O, *et al.*** The combinatorial activities of Nkx2.5 and dHAND are essential for cardiac ventricle formation. *Dev Biol.* 2001; 239: 190–203.
21. **Srivastava D, Thomas T, Lin Q, *et al.*** Regulation of cardiac mesodermal and neural crest development by the bHLH transcription factor, dHAND. *Nat Genet.* 1997; 16: 154–60.
22. **Morikawa Y, Cserjesi P.** Cardiac neural crest expression of Hand2 regulates outflow and second heart field development. *Circ Res.* 2008; 103: 1422–9.
23. **Ritter O, Haase H, Schulte HD, *et al.*** Remodeling of the hypertrophied human myocardium by cardiac bHLH transcription factors. *J Cell Biochem.* 1999; 74: 551–61.
24. **Shen L, Li XF, Shen AD, *et al.*** Transcription factor HAND2 mutations in sporadic Chinese patients with congenital heart disease. *Chin Med J.* 2010; 123: 1623–7.
25. **Ovcharenko D, Kelnar K, Johnson C, *et al.*** Genome-scale microRNA and small interfering RNA screens identify small RNA modulators of TRAIL-induced apoptosis pathway. *Cancer Res.* 2007; 67: 10782–8.
26. **Abell AN, Rivera-Perez JA, Cuevas BD, *et al.*** Ablation of MEKK4 kinase activity causes neurulation and skeletal patterning defects in the mouse embryo. *Mol Cell Biol.* 2005; 25: 8948–59.
27. **Mazerbourg S, Bouley DM, Sudo S, *et al.*** Leucine-rich repeat-containing, G protein-coupled receptor 4 null mice exhibit intrauterine growth retardation associated with embryonic and perinatal lethality. *Mol Endocrinol.* 2004; 18: 2241–54.
28. **Briegel KJ, Baldwin HS, Epstein JA, *et al.*** Congenital heart disease reminiscent of partial trisomy 2p syndrome in mice transgenic for the transcription factor Lbh. *Development.* 2005; 132: 3305–16.